

# Electrochemical Oxidation of Hydrogen Sulfide in Polluted Brines Using Porous Graphite Electrodes under Geothermal Conditions

A M El-Shamy<sup>1\*</sup>, F M Alkharafi<sup>2</sup>, R M Abdallah<sup>2</sup>, I M Ghayad<sup>2</sup>

<sup>1</sup>Department of Physical Chemistry, Electrochemistry and Corrosion Lab, National Research Centre, 12622, Dokki, Cairo, Egypt

<sup>2</sup>Department of Chemistry, Faculty of Science, Kuwait University, Safat 13060, Kuwait

\*Correspondence to: A M El-Shamy, elshamy10@yahoo.com

Accepted: September 10, 2010; Published online: October 28, 2010

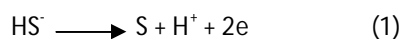
## Abstract

Hydrogen sulfide contaminates the geothermal brines that are encountered in the drilling of wells. It promotes the corrosion of the drilling equipment, pipelines, vessels, forms sulfide scales, which plug tubulars, and degrades the quality of the produced oil. This work aims to study the feasibility of electrochemical removal of H<sub>2</sub>S from such brines by anodic oxidation. Porous graphite electrode was used to achieve electrochemical oxidation of sulfide ions in chloride brines in an autoclave under high temperature and pressure. The X-ray photoelectron spectroscopy (XPS) and Energy Dispersive Spectroscopy (EDS) proved that sulfur was identified as the final reaction product under various potentials and temperatures. In low temperature, the sulfur was detected on the electrode surface, while in high temperature the resulting sulfur flows out in the electrolyte so that it is not detected on the electrode surface. The rate of sulfide oxidation depends on the potential, temperature and the sulfide concentration. The obtained limiting currents are lower than those predicted from mass transfer correlations, which result from the effects of the deposited sulfur on the internal surface of the porous graphite electrode. The large internal surface area of the used electrodes improved the removal efficiency of sulfide ions and this is very clearly noticed from the current transient's results. In high temperature, the limiting current is re-increased due to the liberation of sulfur from the electrode surface, which reactivates electrode surface and the rate of oxidation is increased again.

**Keywords:** Electrochemical oxidation; hydrogen sulfide; porous graphite electrodes; XPS; sulfur; high temperature; high pressure.

## 1. Introduction

Hydrogen sulfide is considered as one of the extremely hazardous substances due to its toxicity for humans and its dangerous effect on metallic materials [1,2]. It promotes the corrosion of metallic materials, which exist specially in oil and gas industry, since it contaminates the geothermal brines [2,3]. It is also present in wastewater of several industries [4-7] and in production of energy [8,9]. There have been many trials to detect, control and/or remove hydrogen sulfide from the polluted media. The efforts have been directed into two methods, precipitation and oxidation. These include chemical, biological and electrochemical oxidation, and adsorption. The scavengers were used to remove the H<sub>2</sub>S, particularly in oil and gas fields. The scavengers such as ZnCO<sub>3</sub>, Na<sub>2</sub>CrO<sub>4</sub>, Fe<sub>3</sub>O<sub>4</sub>, etc are well known for removing hydrogen sulfide from industrial polluted water. The amount of scavengers depends on the level of sulfide content and the properties of the fluid [10-13]. The used scavengers are very expensive and cause environmental pollution. Electrochemical oxidation is an attractive technique for sulfide ion removal. The oxidation of sulfide is attributed to formation of less toxic products [14-16]. The oxidation reaction on the electrode can be represented by:



The anodic oxidation might also be pursued as a means of using H<sub>2</sub>S as a fuel in fuel cells, obtaining sulfur from sour gas or for the sole purpose of ridding the media of H<sub>2</sub>S and its effects [17-19]. The elemental sulfur from sulfide oxidation accumulates on the electrode surface and so it passivates progressive decay of its activity. The sulfur is highly reactive and has many oxidation states, so it is expected to give polysulfides, elemental sulfur or oxysalts such as thiosulfates and sulfates as reaction products [20,21].

The experiments were performed under conditions of high temperature and pressure, which simulates the geothermal fluids but the range of temperature exceeds the melting point of sulfur (115°C). The previous condition required a closed system due to the temperature under experiment being higher than the boiling point of water, so autoclave was used to give the required conditions of temperature and pressure. The porous electrodes possess some attractive features for this purpose due to high specific surface

areas, and can be operated continuously [22,23]. The oxidation of the sulfide ions to produce elemental sulfur at high temperature and pressure gives soluble reaction products; hence, this method can be applied continuously for removing sulfide ions from geothermal fluid. If this technique can be achieved, it can provide an easy and safe method for removing sulfide ions from contaminated brines. This technique can be linked to wastewater treatment, e.g. for the recovery of metal ions [24-34], the destruction of organic and inorganic wastes [35-38], the removal of dissolved oxygen [39], the production of polysulfides from white



liquor [40], the storage of energy [41], the formation of hydrogen peroxide [42] and the recovery of bromine [43,44]. The oxidation of sulfide ions was carried out by using pyrolytic graphite in stagnant conditions, the sulfur was detected on the electrode surface at room temperature, and there is no detection at high temperatures more than its melting point [45]. The objective of this paper is to investigate the capability of achievement of the anodic oxidation of sulfide ions using porous electrodes in batch condition and to assess the effects of some operating parameters on the rate of oxidation.

## 2. Methods

Working electrodes were prepared from carbon felt obtained from Alfa Aesar. It has a thickness of 6.35 mm, a density of  $0.076 \text{ gcm}^{-3}$  and a BET area of  $1.61 \text{ m}^2\text{g}^{-1}$ . All measurements were performed in a supporting electrolyte of 3.5% NaCl containing 0.01 M sodium sulfide. The test solutions were prepared from deionized water and analytical grade chemicals. The cell was equipped with a platinum wire counter electrode positioned downstream, facing porous electrode. Experiments were performed in a Teflon cell contained in an autoclave made from 316 L stainless steel. The autoclave is composed of a main body (Figure 1), and the main body houses the PTFE electrolytic cell. The head of the autoclave has four more openings for a thermocouple and contacts to the working, counter and reference electrodes. To ensure gas-tight sealing of the head onto the autoclave, the head was machined to accommodate two o-rings. Six threaded openings accommodate the studs, which attach the two parts together. The electrolytic cell was fabricated from a block of PTFE to fit tightly in the main body of the autoclave. Figure 1 shows the autoclave and the used Teflon cell and the cell is also composed of a main body which contains the salt solution and a cover. After the cell was assembled and the autoclave sealed, it was placed in a specially designed electric furnace equipped with a temperature regulator and the temperature of the electrolyte was controlled to  $\pm 1^\circ \text{ C}$ . Attainment of constant temperature required about 3 hours. Electrochemical measurements were performed using a Gamry PC4/750 Potentiostat. The potential was scanned from cathodic towards anodic potentials against an Ag/AgCl reference electrode. The porous graphite electrodes were subjected to surface analysis by using a scanning electron microscope (JSM-6300JEOL) and an X-ray photoelectron spectrometer (XPS), FISON Instruments, Model ESCA-lab 200 (VG instruments). After the experiment, rotary vapor instrument was used to evaporate the electrolyte and the residual powder is applied for detection of sulfur by XPS and EDS techniques.

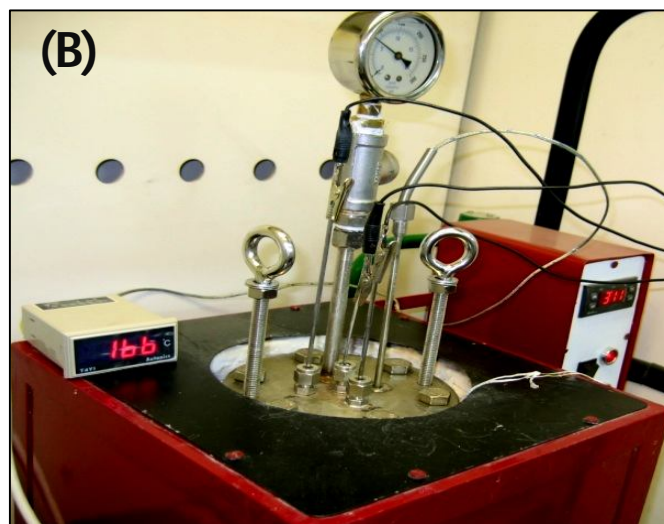


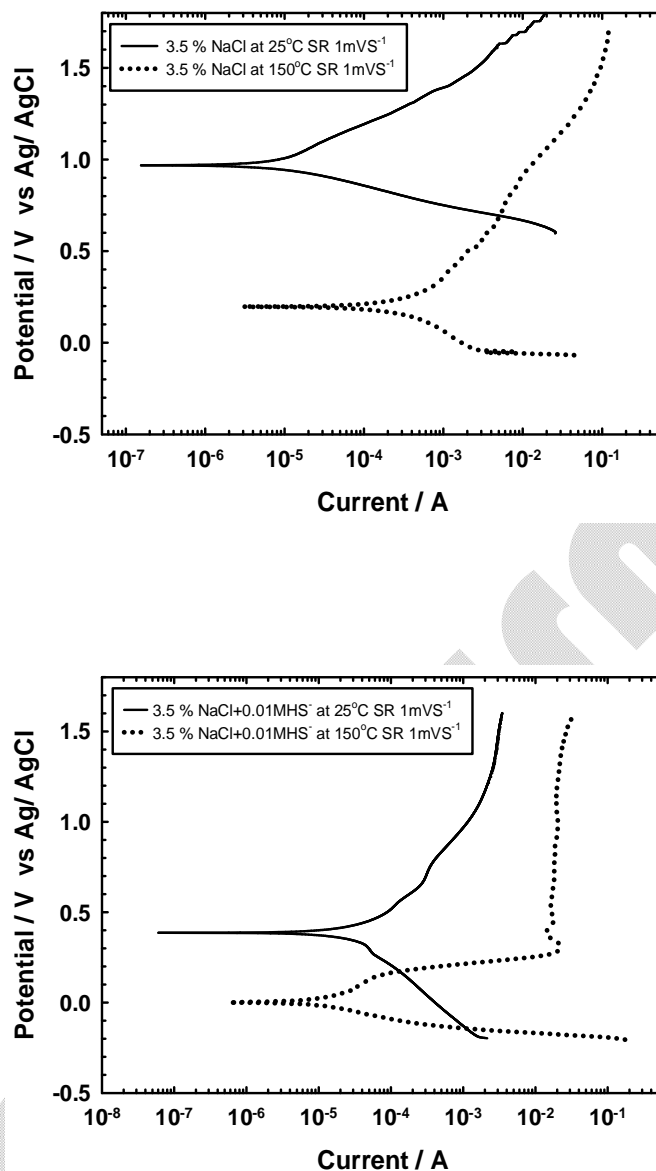
**Figure 1:** (A) Shows the autoclave and the used Teflon cell. (B) Represents the sealed autoclave placed in a specially designed electric furnace equipped with a temperature regulator.

### 3. Results and Discussion

#### 3.1 Electrochemical measurements

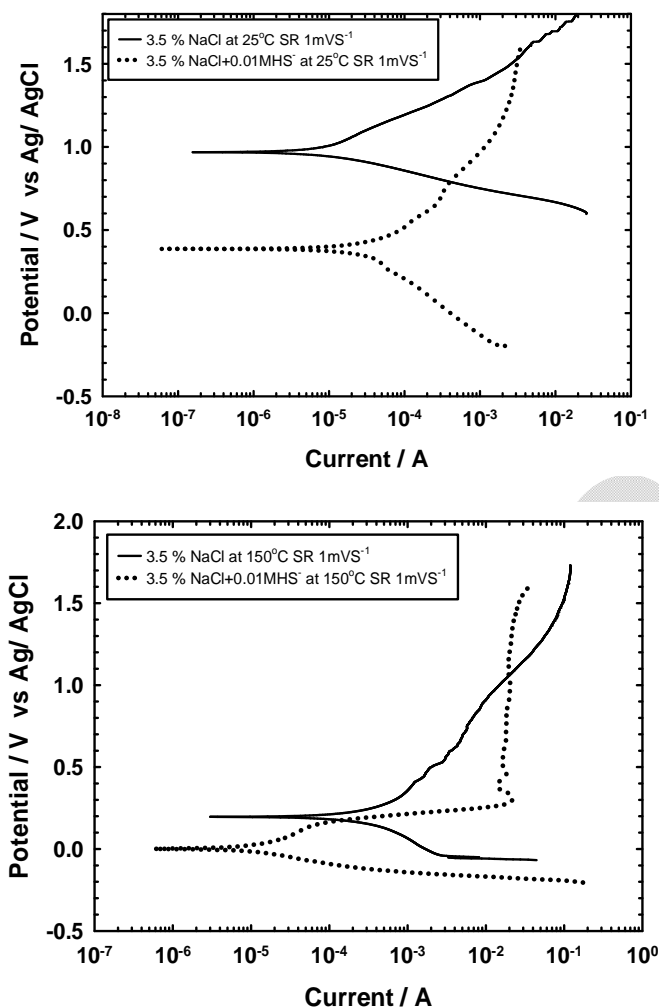
Figure 2a illustrates the effect of temperature on the potentiodynamic current-potential relations obtained on an electrode operated at 3.5 % NaCl at 25°C and 150°C measured at scan rate of 1 mVs<sup>-1</sup>. The upper part of the curve, at the more noble potentials, describes anodic oxidation while the lower part refers to cathodic reduction. The two parts fall on either side of the open circuit potential. The anodic current increases gradually with potential reaching a well-defined limiting value, 20 and 120 mA at 25°C and 150°C respectively. The magnitude of limiting current (*i*<sub>L</sub>) increases with the rise of the temperature up to 6 times, which indicates that the reaction rate is affected by the temperature of the electrolyte. The obtained result shows that the limiting current is reached at potentials a few hundred mV more noble than the open circuit potential, which indicates that the process is associated with significant levels of electrochemical polarization.

Figure 2b shows the effect of temperature on the potentiodynamic current-potential relations obtained on an electrode operated at 3.5 % NaCl + 0.01M HS<sup>-</sup> at 25 ° C and 150° C measured at scan rate of 1 mVs<sup>-1</sup>. The anodic current increases gradually with potential reaching a well defined limiting value, 3 and 30 mA at 25 ° C and 150° C respectively. The magnitude of limiting current (*i*<sub>L</sub>) increases with the temperature rising 10 times, which indicates that the reaction rate is affected by the temperature of the electrolyte and presence of sulfide ions. The obtained result proved that the electrochemical oxidation of sulfide ions is attributed to electrochemical polarization on the electrode surface.



**Figure 2 (a, b):** Effect of temperature on current-potential relation of the porous graphite electrode at a voltage scanning rate of  $1 \text{ mVs}^{-1}$  in (a) 3.5% NaCl only and (b) 3.5% NaCl + 0.01 M  $\text{HS}^-$  at  $25^\circ \text{C}$  and  $150^\circ \text{C}$ .

Figure 3a and b illustrate the effect of sulfide ions on the current-potential relation at  $25^\circ \text{C}$  and  $150^\circ \text{C}$  and it is well known that the limiting current is increased in presence of sulfide ions at low and high temperature, which indicates that the reaction is going in the direction of oxidation of sulfide ions. The obtained results prove that the limiting current is affected by increasing temperature and the lowering of limiting current at low temperature is attributed to the formation of elemental sulfur on the porous electrode surface, which lowers the rate of reaction due to the passivation of electrode surface. In high temperature, the limiting current is re-increased due to the liberation of sulfur from the electrode surface as the used temperature is higher than the melting point of sulfur ( $115^\circ \text{C}$ ) that reactivates electrode surface and the rate of oxidation is increased again.

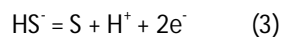


**Figure 3 (a, b):** Effect of sulfide ions on current-potential relation for the porous graphite electrode at a voltage scanning rate of  $1 \text{ mVs}^{-1}$  in 3.5% NaCl only and 3.5% NaCl +0.01 M  $\text{HS}^-$  at (A)  $25^\circ \text{C}$  (B)  $150^\circ \text{C}$ .

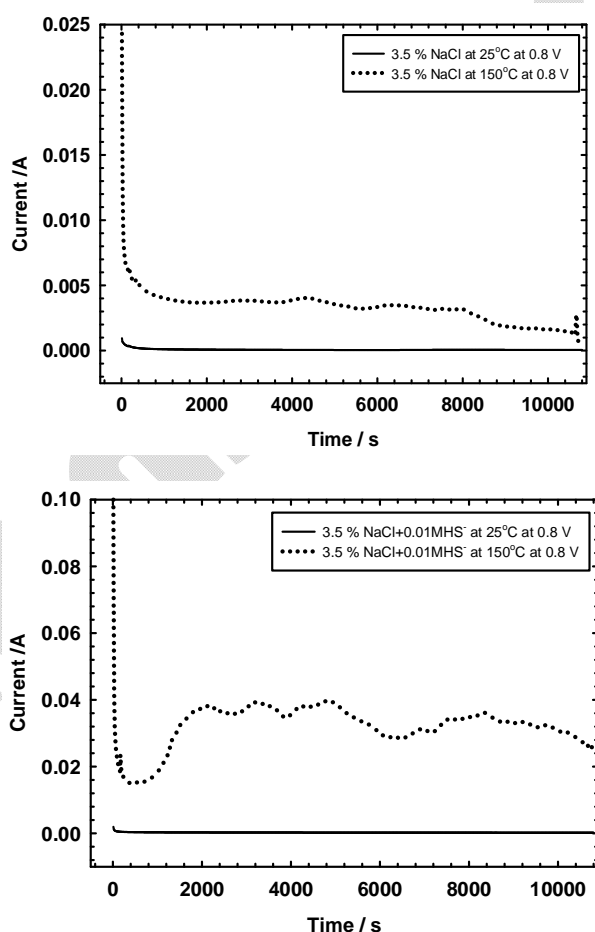
Figure 4a illustrates the current transients supported by the porous graphite electrode at a potential of 0.8 V (Ag/AgCl) in 3.5% NaCl at  $25^\circ \text{C}$  and  $150^\circ \text{C}$ . The results show that the current is increased with increasing temperature and it is previously noticed from the potentiodynamic results. The increasing current shows higher value, more than that obtained in case of presence of sulfide, and the results are shown in Figure 4b. The results indicate that the current depends on the existence of sulfide and the temperature of the electrolyte. There is no gradual decrease of current with time, which attributed to the melting of elemental sulfur from the internal surface of the porous electrode and so the reaction rate is continuously activated. This indicates that the porous electrode has a higher capacity for removing the sulfide ions from the polluted brines. The potential distribution within a porous electrode is non-uniform. In view of the three dimensional nature of the porous electrodes, there is always a potential shift within the electrode, the magnitude of which depends on the resistivity of the pore electrolyte ( $\rho$ ), the thickness of the electrode ( $L$ ) and the distribution of the current produced within the electrode. The potential distribution can only be obtained upon development of a mathematical model of the process and solution of the model equation [31–33]. By assuming that the current ( $i$ ) is generated entirely near the bottom face of the porous electrode, the estimation of the maximum possible shift in potential  $\Delta E_{\text{max}}$  can be obtained from the following equation:

$$\Delta E_{\text{max}} = iL\rho/a \quad (2)$$

By using  $L = 0.635$  cm,  $\rho = 22$  ohm cm and  $a = 5.3$  cm<sup>2</sup>, a value of  $\Delta E$  (max)  $\approx 100$  mV is obtained. For a current of 10 mA,  $\Delta E$  (max) amount to only 26.4 mV. Normally, the actual potential drop is much less than  $\Delta E$  (max). It is found that under certain conditions about 80% of the current was generated in the top 20% of the thickness of the porous electrode [32], and the actual potential shift is only about 20% of the value given by Equation 2. For a current at 2000 s in Figure 4 (a,b) amount to only 4 and 40 mA or less, so the potential at various locations inside the porous electrode is less noble than the 400 mV (Ag/AgCl) at the top surface by an amount that ranges from a few to 100 mV, which is considered as a limiting value. It was shown elsewhere that elemental sulfur formed on solid graphite electrodes at potentials as low as 180 mV (SCE) [16]. This indicates that the potential inside the porous electrode is favorable for the formation of elemental sulfur. Equation 3 shows the formation of elemental sulfur:



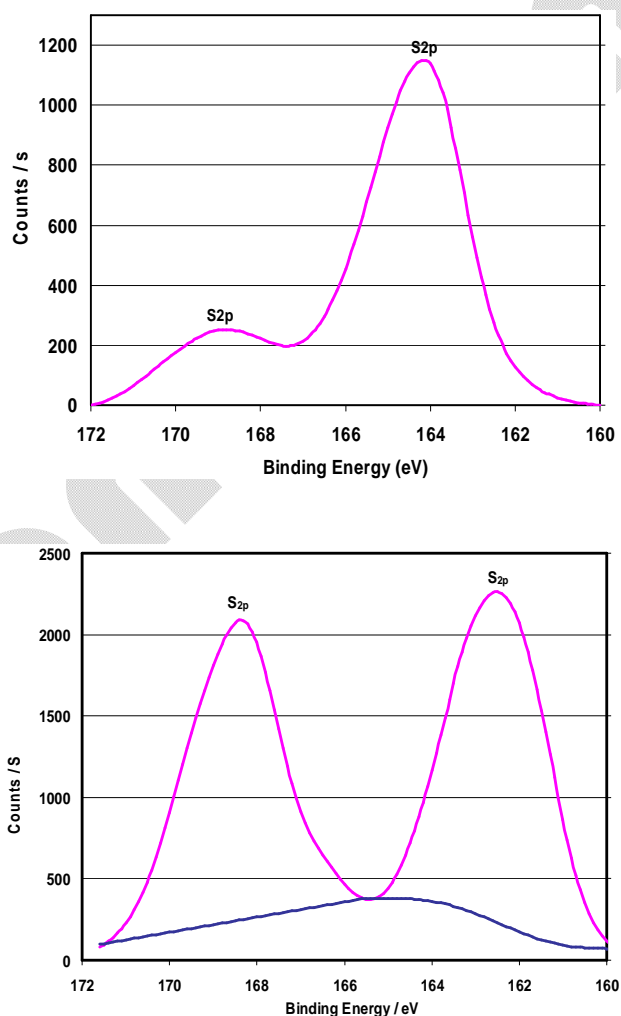
The sulfur has high reactivity and many oxidation states, which affects the electrochemical behavior of the sulfide ions in aqueous media [20, 21]. As shown above, the rate of the process is affected by charge transfer across the interface, which is also affected by the diffusion through the electrolyte towards the graphite surface. Under the ambient conditions, the stable form S<sub>8</sub> is formed by the polymerization of atomic sulfur.



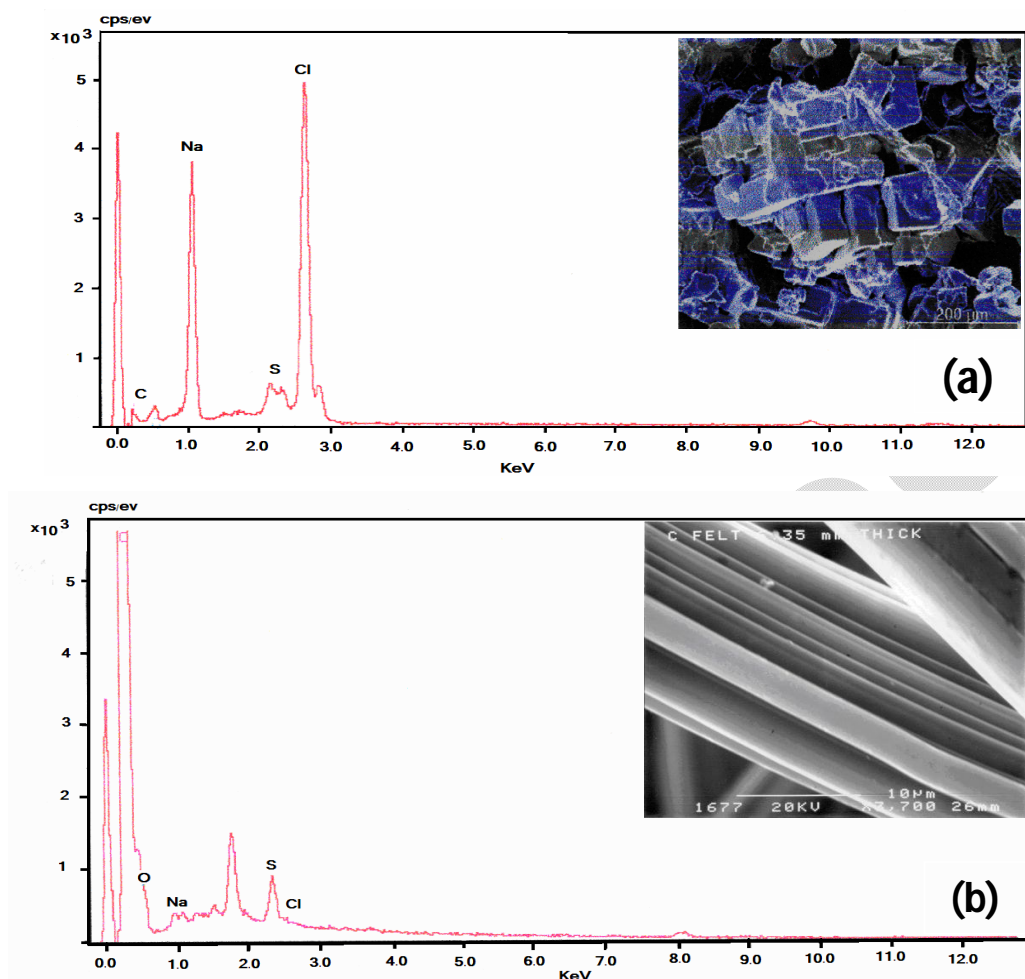
**Figure 4 (a, b):** Current transients supported by the porous graphite electrode at a potential of 0.8 V (Ag/AgCl) in (a) 3.5% NaCl at 25° C and 150° C, and (b) 3.5% NaCl+0.01 M HS<sup>-</sup> at 25° C and 150° C.

### 3.2 Characterization of the reaction products

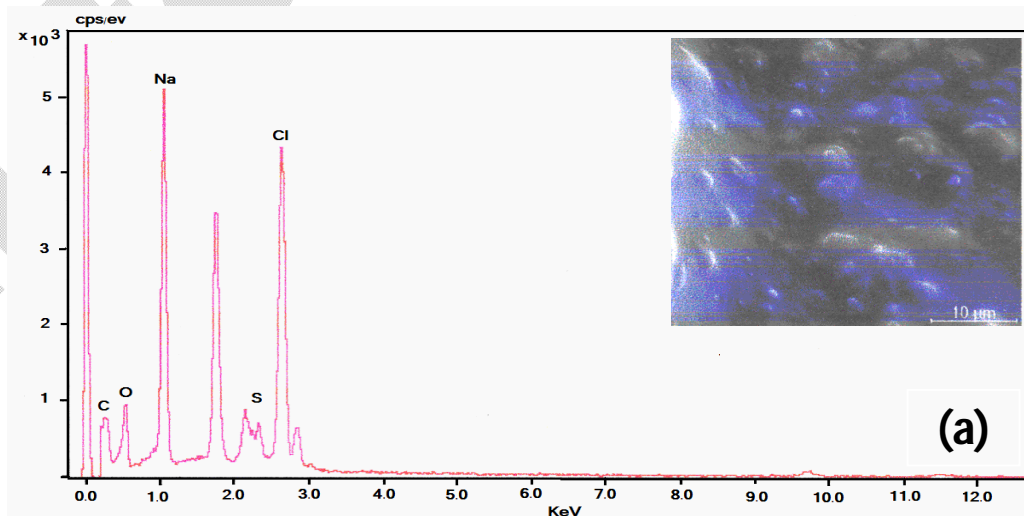
The electrode surface and the residual powder of the used electrolyte were inspected microscopically by using SEM and subjected to XPS and EDS spectrum after performing the electrolysis at 25° C and 150° C. Figure 5a shows an XPS spectrum of the residual powder of the used electrolyte after evaporation of the residual polluted brine by using rotary vapor device. The solution containing 3.5% NaCl and 0.01M HS<sup>-</sup> was subjected to polarization by using porous graphite electrode at 0.8 V (Ag/AgCl) for 3 h at 25° C. It is well-known that the elemental sulfur appears at the values ranging from 163.6 to 164.2 eV [46]. Figure 5a shows a prominent S2p peak at a binding energy of 164.8 eV, which is attributed to the presence of elemental sulfur at intensity of about 1080 CPS. The results prove that the obtained intensity is lower than in case of high temperature and the obtained species is different from the low temperature. Figure 5b illustrates two prominent peaks at about 161.8 eV and 168.5 eV corresponding to the sulfide ions and sulfate ions, respectively [45,47] at intensity of 2300 and 2100, respectively. The results prove that at 25° C not all of formed elemental sulfur is present in the residual powder, but some of it is also present on the electrode surface. Further confirmation of these findings is provided by the results of SEM and EDS measurements on powder and porous graphite electrode. Figure 6a shows the SEM and EDS for the residual powder of the used electrolyte, which was polarized by porous graphite electrode for 3 h at 25° C. The obtained result shows strong signal at about 2.5 KeV, which indicates to the elemental sulfur. Figure 6b shows the SEM and EDS for the porous electrode surface in the conditions similar to Figure 6a and we note that a clear signal at about 2.5 KeV, which is ascribed to sulfur.



**Figure 5 (a, b):** XPS spectrum of the residual powder of an evaporated used electrolyte by rotary vapor device, the electrolyte is subjected for polarization at a potential of 0.8 V (Ag/AgCl) by using porous graphite electrode for 3 h, in presence of 3.5% NaCl + 0.01 M HS<sup>-</sup> at (a) 25° C and (b) 150° C.



**Figure 6 (a, b):** (a) SEM and EDS of powder of evaporated used electrolyte containing 0.01M  $\text{HS}^-$  at a potential of 0.8 V(Ag/AgCl), which was polarized by porous graphite electrode for 3 h at 25° C. (b) SEM and EDS of fibers of porous graphite electrode after it was polarized in a solution containing 0.01M  $\text{HS}^-$  at a potential of 0.8 V(Ag/AgCl) for 3 h at 25° C.



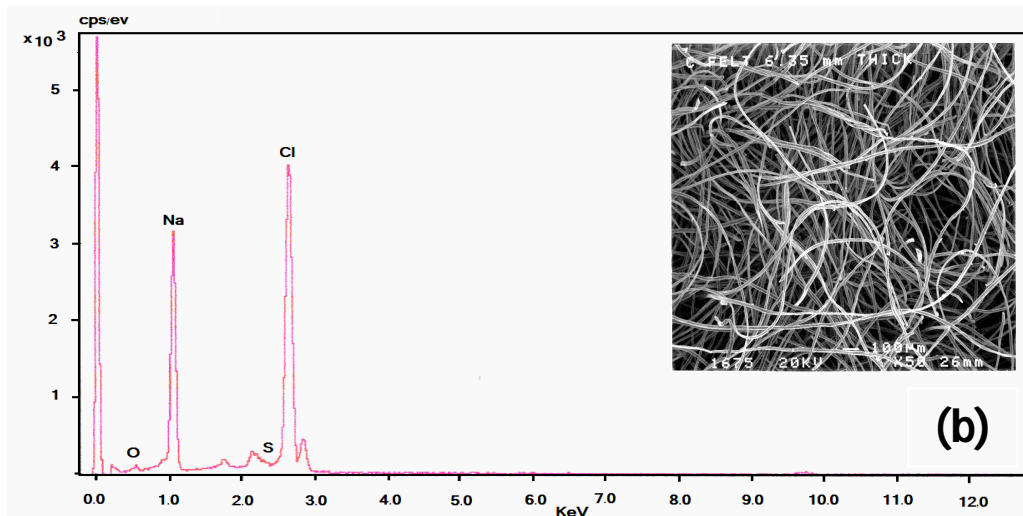


**Figure 7 (a, b):** (a) SEM and EDS of powder of evaporated used electrolyte containing  $0.01\text{M HS}^-$  at a potential of  $0.8\text{ V(Ag/AgCl)}$ , which was polarized by porous graphite electrode for 3 h at  $150^\circ\text{C}$ . (b) SEM and EDS of fibers of porous graphite electrode after it was polarized in a solution containing  $0.01\text{M HS}^-$  at a potential of  $0.8\text{ V(Ag/AgCl)}$  for 3 h at  $150^\circ\text{C}$ .

Figure 6 (a, b) give a second proof for the previously obtained results. The reaction rate at room temperature is lower than at high temperature and this is clearly noticed from the intensity of the XPS spectrum. Figure 5b shows the XPS spectrum of the residual powder of the used electrolyte in the previous conditions, but at  $150^\circ\text{C}$ , which elucidates two clear peaks for sulfide and sulfate ions with higher intensity than the produced peak in Figure 5a. On the other hand, the thermodynamic calculations predict that elemental sulfur can produce soluble oxyanions, and in principle, undergo further oxidation [20, 21]. Furthermore, elemental sulfur can also dissolve in the presence of sulfide ions to give several polysulfides [14, 15, 48]. The EDS of porous graphite electrode shows very small signal at 2.5 KeV, which proves that the presence of elemental sulfur on the electrode surface is negligible at high temperature (Figure 7b) and that, is in agreement with the obtained results. That is why the reaction rate is approximately constant and the majority of sulfur species is present in the residual powder (Figure 7a), so this process can be used in the field continuously for removing the sulfide ions through the electrochemical oxidation by using porous graphite electrode under severe conditions of temperature and pressure.

#### 4. Conclusion

The present work revealed that in geothermal conditions it is possible to oxidize sulfide ions directly from polluted chloride brines into elemental sulfur at porous graphite electrodes. The oxidation process is controlled by both charge transfer at the interface and mass transfer within the electrolyte. The results show that at low temperature the elemental sulfur passivates the electrode surface; this was attributed to the passivating effects of the deposited sulfur inside the porous medium, which subsequently decreases the rate of the oxidation process, which is clearly noticed from the magnitude of limiting current. The porous graphite electrode has high capacity for removing sulfide ions, which is attributed to its large internal surface area. The oxidation of sulfide ions to sulfate ions serves the objective of this work by decreasing the concentration of sulfide in the brine. Furthermore, in case of over oxidation of the brine, the chlorine gas is produced, this has a favorable bactericidal activity, that inhibits the sulfate reducing bacteria. The reaction rate of the sulfide removal efficiency increases with temperature.

#### Competing Interests

The authors declare that they have no competing interests.

### Authors' Contributions

AME dealt with preparation of the manuscript and data analysis; FMA was principal investigator of the project and supervised preparation of the manuscript; RMA cooperated with principal investigator and supervised the experimental work; IMG assisted with experimental work and carried out the project.

### Acknowledgement

The authors gratefully acknowledge financial support of this work by the Research Administration of Kuwait University, under Grant Number SC04/99. They also thank the Electron Microscopy Unit for performing SEM and EDS measurements.

### References

- [1] United States Environmental Protection Agency, 1988. Extremely Hazardous Substance. Superfund Chemical Profiles, CAS Registry Number 7783-06-4, Vol. 1, Noyes Data Corporation, New Jersey.
- [2] Tuttle RN, Kane RD, 1981. H<sub>2</sub>S Corrosion in Oil and Gas Production. National Association of Corrosion Engineers, Houston, Texas.
- [3] Garverick L, 1994. Corrosion in the Petrochemical Industry. ASM International, Metals Park, Ohio, p. 259.
- [4] Rajalo G, Petrovskaya T, 1996. Selective Electrochemical Oxidation of Sulfides in Tannery Wastewater. *Environmental Technology*, 17: 605-612.
- [5] Rao NN, Somasekhar KM, Kaul SN, Szpyrkowicz L, 2001. Electrochemical oxidation of tannery wastewater. *Journal of Chemical Technology and Biotechnology*, 76: 1124-1131.
- [6] Szpyrkowicz L, Kaul SN, Neti RN, 2005. Tannery wastewater treatment by electro-oxidation coupled with a biological process. *Journal of Applied Electrochemistry*, 35: 381-390.
- [7] Behm M, Simonsson D, 1997. Graphite as anode material for the electrochemical production of polysulfide ions in white liquor. *Journal of Applied Electrochemistry*, 29: 521-524.
- [8] Kagel A, 2008. The State of Geothermal Technology. Part II: Surface Technology, The Department of Energy, Washington D. C., p 5.
- [9] Clauser C, 2006. Geothermal Energy. In: K. Heinloth (ed.), *Landolt - Börnstein, Group VIII: Advanced Materials and Technologies, Vol. 3: Energy Technologies, Subvol. C: Renewable Energies*, Springer Verlag, Heidelberg-Berlin, 493-604, p 98.
- [10] Garrett RL, Clark RK, Carney LL, Granthm CK, 1997. Chemical Scavengers for Sulfides in Water-Based Drilling Fluids, *SPE Reprint Series*, 44: 170.
- [11] Singh AK, Kohil BS, Wendt RP, 1989. Handling hydrogen sulfide in drilling fluids. *World Oil*, 209: 99; *ibid* 209: 77.
- [12] Al-Humaidan AY, Nasr El-Din HA, 1999. Optimization of Hydrogen Sulfide Scavengers used during Well Stimulation in *Proceedings of the SPE International Symposium on Oilfield Chemistry*.
- [13] Chr. Schorling P, Brauchle M, 2001. Application of Hydrogen Sulfide Scavengers in the Oil and Gas Field. *Erdoel Ergas Kohle/EKEP*, 117: 78.

- [14] Anani A, Mao Z, White RE, Srinivasan S, Appleby AJ, 1990. Electrochemical Production of Hydrogen and Sulfur by Low Temperature Decomposition of Hydrogen Sulfide in an Aqueous Alkaline Solution. *Journal of Electrochemical Society*, 137: 2703-2709.
- [15] Anani A, Mao Z, White RE, Srinivasan S, Appleby AJ, 1991. Electrochemical Process for the Decomposition of Hydrogen Sulfide in an Aqueous Alkaline Solution. *Journal of Electrochemical Society*, 138: 1299.
- [16] Ateya BG, Al-Kharafi FM, 2002. Anodic oxidation of sulfide ions from chloride brines. *Electrochemistry Communications*, 4: 231-238.
- [17] Ateya BG, AlKharafi FM, Alazab AS, Abdullah AM, 2007. Kinetics of the electrochemical deposition of sulfur from sulfide polluted brines. *Journal of Applied Electrochemistry*, 37: 395-404.
- [18] Petrov K, Srinivasan S, 1999. Low temperature removal of hydrogen sulfide from sour gas and its utilization for hydrogen and sulfur production. *International Journal Hydrogen Energy*, 21: 163-169.
- [19] Bockris JOM, Shahid Khan UM, 1993. *Surface Electrochemistry: A Molecular Level Approach*. (Plenum Press, London) p. 541, 951.
- [20] Bard AJ, Parsons R, Jordan J, 1985. *Standard Potentials in Aqueous Solutions*. Editor: Marcel Dekker, Inc, New York, p. 94.
- [21] Valensi G, van Muylder J, Pourbaix M, 1974. In M. Pourbaix (Ed.), *Atlas of Electrochemical Equilibria in Aqueous Media* (National Association of Corrosion Engineering, Texas), p. 545.
- [22] Newman SJ, 1991. *Electrochemical Systems*. 2nd edn, Prentice Hall, Engle Wood Cliffs, New Jersey, p. 487.
- [23] Deab MS, Saleh MM, El-Anadouli BE, Ateya BG, 1999. Electrochemical Removal of Lead from Flowing Electrolytes Using Packed Bed Electrodes. *Journal of Electrochemical Society*, 146: 208-213.
- [24] Scott K, Paton EM, 1993. An analysis of metal recovery by electrodeposition from mixed metal ion solutions—part II. Electrodeposition of cadmium from process solutions. *Electrochimica Acta*, 38: 2191-2197.
- [25] Ponce De Leon C, Pletcher D, 1996. The removal of Pb(II) from aqueous solutions using a reticulated vitreous carbon cathode cell—the influence of the electrolyte medium. *Electrochimica Acta*, 41: 533-541.
- [26] Bennion DN, Newman J, 1972. Electrochemical removal of copper ions from very dilute solutions. *Journal of Applied Electrochemistry*, 2: 113-122.
- [27] Stankovic VD, Wragg AA, 1995. Modelling of time-dependent performance criteria in a three-dimensional cell system during batch recirculation copper recovery. *Journal of Applied Electrochemistry*, 25: 565-573.
- [28] Bisang JM, 1996. Theoretical and experimental studies of the effect of side reactions in copper deposition from dilute solutions on packed-bed electrodes. *Journal of Applied Electrochemistry*, 26: 135-142.
- [29] van Zee J, Newman J, 1977. Electrochemical Removal of Silver Ions from Photographic Fixing Solutions Using a Porous Flow-Through Electrode. *Journal of Electrochemical Society*, 124: 706-708.
- [30] Wang J, Dewald HM, 1983. Deposition of Metals at Flow-Through Reticulated Vitreous Carbon Electrodes Coupled with On-line Monitoring of the Effluent. *Journal of Electrochemical Society*, 130: 1814.
- [31] Saleh MM, Weidner JW, Ateya BG, 1995. Electrowinning of Non-Noble Metals with Simultaneous Hydrogen Evolution at Flow through Porous Electrodes. I. Theoretical. *Journal of Electrochemical Society*, 142: 4113-4121.
- [32] Saleh MM, Weidner JW, Ateya BG, 1995. Electrowinning of Non-Noble Metals with Simultaneous Hydrogen Evolution at Flow Through Porous Electrodes. II. Experimenta. *Journal of Electrochemical Society*, 142: 4122-4128.

- [33] Saleh MM, Weidner JW, Ateya BG, 1997. Electrowinning of Non-Noble Metals with Simultaneous Hydrogen Evolution at Flow Through Porous Electrodes. III. Time Effects. *Journal of Electrochemical Society*, 144: 922-927.
- [34] Hatfield TL, Kelven TI, Pierce DT, 1996. Electrochemical remediation of metal-bearing wastewaters Part I: Copper removal from simulated mine drainage waters. *Journal of Applied Electrochemistry*, 26: 567-574.
- [35] Conway BE, Ayranci E, Al-Maznai H, 2001. Use of quasi-3-dimensional porous electrodes for adsorption and electrocatalytic removal of impurities from wastewaters. *Electrochimica Acta*, 47: 705-718.
- [36] Hofseth CS, Chapman TW, 1999. Electrochemical destruction of dilute cyanide by copper-catalyzed oxidation in a flow-through porous electrode. *Journal of Electrochemical Society*, 146: 199-207.
- [37] Ponce de Leon C, Pletcher D, 1995. Removal of formaldehyde from aqueous solution via oxygen reduction using reticulated vitreous carbon cathode cell. *Journal of Applied Electrochemistry*, 25: 307-314.
- [38] Cagnet P, Berlan J, Lacot G, Fabre PL, Jud JM, 1996. Application of metallic foams in an electrochemical pulsed flow reactor Part II: Oxidation of benzyl alcohol. *Journal of Applied Electrochemistry*, 26: 631-637.
- [39] Kinzel P, Lintz HG, Gaudebert P, Bousquet V, Lopicque F, Valentin G, 2002. Electrocatalytic removal of dissolved oxygen from seawater in a packed-bed electrode. *Journal of Applied Electrochemistry*, 32: 951-960.
- [40] Behm M, Simonsson D, 1997. Electrochemical Production of Polysulfides and Sodium-Hydroxide from White Liquor. 2. Electrolysis in a Laboratory-Scale Flow Cell. *Journal of Applied Electrochemistry*, 27: 519-528.
- [41] Lessner PM, McLarnon FR, Winnick J, Cairns EJ, 1992. Aqueous polysulphide flow-through electrodes: effects of electrocatalyst and electrolyte composition on performance. *Journal of Applied Electrochemistry*, 22: 927-934.
- [42] Huissoud A, Tissot P, 1999. Electrochemical reduction of 2-ethyl-9,10-anthraquinone (EAQ) and mediated formation of hydrogen peroxide in a two-phase medium Part II: Production of alkaline hydrogen peroxide by the intermediate electroreduction of EAQ in a flow-by porous electrode in two-phase liquid-liquid flow. *Journal of Applied Electrochemistry*, 29: 17-25.
- [43] Jian Q, Savinell RF, 1993. Analysis of flow-through porous electrode cell with homogeneous chemical reactions: application to bromide oxidation in brine solutions. *Journal of Applied Electrochemistry*, 23: 873-886.
- [44] Jian Q, Savinell RF, 1993. Development of the flow-through porous electrode cell for bromide recovery from brine solutions. *Journal of Applied Electrochemistry*, 23: 887-896.
- [45] Ateya BG, Alkharafi FM, El-Shamy AM, Saad AY, Abdalla RM, 2009. Electrochemical desulphurization of geothermal fluids under high temperature and pressure. *Journal of Applied Electrochemistry*, 39: 383-389.
- [46] Gerson AR, Bredow T, 2000. Interpretation of sulfur (2p) XPS spectra by means of ab initio calculations. *Surface and Interface Analysis*, 29: 145-150.
- [47] Briggs D, Seah MP, 1990. *Practical surface analysis*. Wiley, New York, p 605.
- [48] Herszage JDM, Afonso S, 2003. Mechanism Of Hydrogen Sulfide Oxidation By Manganese (IV) Oxide In Aqueous Solutions. *Langmuir*, 19: 9684-9692.